Time-resolved, in situ X-ray diffraction studies of intercalation in lamellar hosts

ARTICLE *in* POLYHEDRON · FEBRUARY 2000

Impact Factor: 2.01 · DOI: 10.1016/S0277-5387(99)00359-9

4 AUTHORS, INCLUDING:

Dermot O'Hare
University of Oxford
392 PUBLICATIONS **10,308** CITATIONS
SEE PROFILE

Andrew M. Fogg
University of Chester
66 PUBLICATIONS **1,758** CITATIONS
SEE PROFILE

Stephen O'Brien
City College of New York
126 PUBLICATIONS **7,787** CITATIONS
SEE PROFILE

PERGAMON

www.elsevier.nl/locate/poly

Polyhedron 19 (2000) 297–305

POLYHEDRON

Time-resolved, in situ X-ray diffraction studies of intercalation in lamellar hosts

Dermot O'Hare *, John S.O. Evans [1], Andrew Fogg, Stephen O'Brien

Inorganic Chemistry Laboratory, South Parks Road, Oxford OX1 3QR, UK

Received 25 April 1999; accepted 29 August 1999

Abstract

Energy dispersive X-ray diffraction (EDXRD) has been used to perform in situ kinetic studies on the intercalation of a range of guest molecules in layered lattices. The kinetics of the intercalation of cations (K^+, PyH^+ ($Py = C_5H_5N$), NMe_4^+) and the long chain ammonium ions $C_{12}TMA$, $C_{16}TMA$, $C_{18}TMA$ ($C_{12}TMA$ = dodecyltrimethylammonium, $C_{16}TMA$ = hexadecyltrimethylammonium and $C_{18}TMA$ = octadecyltrimethylammonium) into crystals of $MnPS_3$ have been determined. These reactions are very fast, and in some cases novel transient phases are observed. The rate of cobaltocene, $Co(\eta\text{-}C_5H_5)_2$, intercalation in layered metal dichalcogenides ZrS_2, 2H-SnS_2, 2H-$SnSe_2$, 2H-TaS_2, 2H-NbS_2, 1T-TaS_2 and TiS_2 has also been investigated. Integrated intensities of the Bragg reflections have been used to determine the extent of reaction (α) versus time for each of these reactions. A number of kinetic models have been considered, including the Avrami–Erofeyev ($m = 1.5$) deceleratory nuclei-growth model and statistical simulation. The concentration and solvent dependence of the rate of $Co(\eta\text{-}C_5H_5)_2$ intercalation into 2H-SnS_2 has also been determined. Surprisingly, we find that the rate of intercalation is invariant to the initial $Co(\eta\text{-}C_5H_5)_2$ concentration over a wide concentration range. The rate of intercalation of the lithium salts (LiX; X = Cl, Br, NO_3 and OH) into Gibbsite (γ-$Al(OH)_3$) giving the layered double hydroxides $[LiAl_2(OH)_6]X \cdot nH_2O$ (X = Cl, Br, NO_3 and OH) and $[LiAl_2(OH)_6]_2SO_4 \cdot nH_2O$ has been studied. The temperature dependence of the rate of intercalation of LiCl yields an activation energy of 27 kJ mol^{-1}. The reaction was also found to be half order with respect to the initial concentration of LiCl. Time-resolved in situ energy dispersive X-ray powder diffraction (EDXRD) spectra have been recorded following the addition of an aqueous solution of hexadecyltrimethylammonium chloride ($C_{16}H_{33}N^+Me_3Cl^- = C_{16}TMACl$) to kanemite ($NaHSi_2O_5 \cdot 3H_2O$). The diffraction data suggest that initially a layered phase forms due to intercalation of the alkylammonium ions which then transforms into a silicate-organic mesophase which is the precursor to the hexagonal mesoporous silicate, FSM-16.

Keywords: In situ X-ray diffraction; Intercalation; Layered compounds; Solid state; Synchrotron radiation

1. Introduction

Some of the earliest and most extensive studies of the kinetics of intercalation reactions were carried out using graphite crystals. For example, classic experiments performed by Hooley and co-workers investigated the gain in weight of a graphite flake under a bromine atmosphere [1,2]. Until recently, only two time-resolved diffraction studies on metal chalcogenide intercalation have been reported [3–7]. The study by Riekel and Schollhorn measured time-resolved neutron diffraction data during the intercalation of 2H-TaS_2 with $NH_3(g)$. However, the available levels of beam flux, whilst high by neutron standards, necessitated either very large sample sizes ($\sim$15 g) or long acquisition times, making a thorough, quantitative study under varying reaction conditions of temperature, concentration and particle size unfeasible. Moreover, because of the large incoherent scattering from hydrogen atoms by neutrons, the samples studied had to be highly deuterated, an expensive and not always achievable prerequisite for other intercalation reactions. Even taking all these previous experiments into consideration, we still have a fairly rudimentary understanding of the intimate mechanism of intercalation reactions. Knowledge of the critical factors which control the rates of these reactions is based on a limited range of experiments. We still commonly use the schematic illustration shown in Fig. 1 to describe these reactions, which undoubtedly greatly oversimplifies the true picture.

In recent years, the technological and experimental advances in energy dispersive powder diffraction (EDXRD) using synchrotron X-ray sources have provided new possi-

* Corresponding author; e-mail: dermot.ohare@chem.ox.ac.uk

[1] Present address: Department of Chemistry, Durham University, Durham DH1 3LE, UK.

0277-5387/00/$ - see front matter
PII S0277-5387(99)00359-9

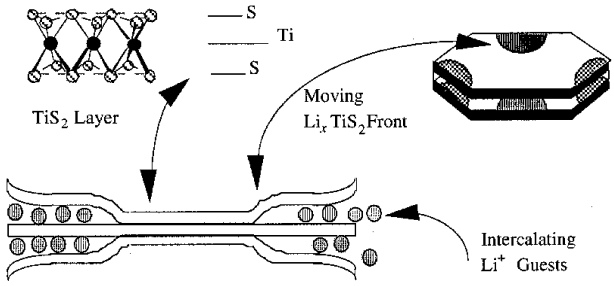

Fig. 1. Schematic representation of the intercalation of a guest into a layered dichalcogenide host lattice.

bilities for the solid state kineticist [8–11]. The markedly higher intensity (several orders of magnitude) over conventional laboratory X-ray sources means that good quality spectra can now be obtained from milligram samples on a time-scale of seconds, making kinetic studies on fast intercalation reactions a realisable goal. We have recently constructed and commissioned a number of environmental cells for measuring time-resolved energy dispersive X-ray diffraction data of intercalation reactions [12–14].

In this paper we will review some of the significant observations we have made to date concerning our investigations into the kinetics of intercalation reactions using in situ, time-resolved X-ray diffraction.

2. Kinetics of intercalation reactions

2.1. Intercalation of cations in metal hexathiohypodiphosphates

The transition metal hexathiohypodiphosphates, MPS_3 (M = Mn, Fe, Ni, Cd), have been shown to intercalate a wide range of guest ions and molecules. In recent years they have been shown by Clement and co-workers to exhibit a unique type of intercalation reaction. MPS_3 (M = Mn, Cd, Fe) reacts spontaneously with aqueous solutions of ionic salts, G^+X^- (where G^+ can range from simple ionic species such as K^+ and NH_4^+ to species as large as, for example, cobaltocenium cations), to give compounds of general formula $Mn_{1-x}PS_3\{G\}_{2x}(H_2O)_y$ [15–17]. In these compounds, charge balance has been maintained by the loss of one Mn^{2+} ion from the intralayer region for every two G^+ ions that are intercalated in the interlayer region.

We have studied the kinetics of K^+, PyH^+ (Py = C_5H_5N), NMe_4^+ and the long chain ammonium ions $C_{12}TMA$, $C_{16}TMA$, $C_{18}TMA$ ($C_{12}TMA$ = dodecyltrimethylammonium, $C_{16}TMA$ = hexadecyltrimethylammonium and $C_{18}TMA$ = octadecyltrimethylammonium) intercalation into sub 90 μm crystals of $MnPS_3$ in water between room temperature and 120°C using time-resolved in situ EDXRD [18]. In a typical experiment, solutions of the appropriate reagents were preheated to the reaction temperature, remotely injected into a 5 ml flask containing the stirred host lattice, and the X-ray diffraction pattern of the resulting suspension monitored as a function of time. Under these conditions the diffraction pattern could be recorded over a 20–4 Å *d*-spacing range in as little as 10 s, allowing the direct observation of the disappearance of the host lattice and growth of the product phase.

Kinetic information was extracted from each experiment by integration of the 001 Bragg reflection using a Gaussian peak fitting routine [19]. The time dependence for pyH^+ intercalation in $MnPS_3$ is shown in Fig. 2. The errors on the integrated areas are small and contained within the data points. The integrated intensities were subsequently converted to the extent of the reaction, α, using the relationship (Eq. (1)):

$$\alpha_{hkl}(t)=\left(\frac{I_{hkl}(t)}{I_{hkl}(t_\infty)}\right) \quad (1)$$

The kinetics of intercalation were analysed following the method of Hulbert, who showed that the general rate expression for nucleation growth reactions developed by Avrami takes the form of Eq. (2) [20–24]. A summary of the least squares fits of such an expression to the experimental data and the rate parameters of the fits are given in Table 1.

$$\ln\frac{1}{1-\alpha}=(kt)^m \quad (2)$$

where α represents the extent of reaction at time *t*.

A number of important conclusions can be drawn from this study. Firstly these intercalation reactions occur extremely rapidly, with half-lives of the order of a minute or less. These exchange intercalation reactions appear to be some of the fastest known molecular intercalation reactions. Secondly the reactions occurred cleanly via a two-phase reactant to product route, and no phenomena such as staging were observed. These systems obey rate expressions similar to those found for the intercalation reactions of other host lattices, and the rate of formation of the product phase and disappearance of the host lattice obey identical rate laws.

The intercalation of dodecyltrimethylammonium bromide ($C_{12}TMABr$) into $MnPS_3$ at 120°C has also been studied using in situ energy dispersive X-ray powder diffraction. The reaction proceeds smoothly and affords a stable crystalline

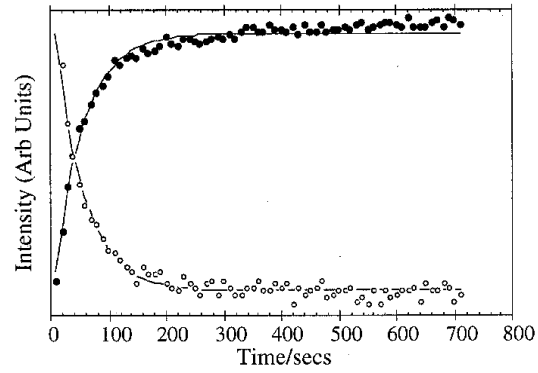

Fig. 2. The time dependence of the intensities of the host (001) (○) and intercalate (001) (●) reflections for the intercalation of pyH^+ by $MnPS_3$ under aqueous conditions at T = 33°C.

Table 1
Kinetic rate parameters for the intercalation of various guest species into some lamellar hosts: experimental rates have been fitted to a rate expression $\alpha = [1 - \exp(-kt)^m]$

Host	Guest	Temperature (°C)	m	k (10^{-3} s^{-1})	$t_{1/2}$ (s)
$MnPS_3$	K^+	33	1.0	12.0	55
$MnPS_3$	pyH^+	33	1.0	20	43
$MnPS_3$	NMe_4^+	51	1.0	88	59
$MnPS_3$	NMe_4^+	60	1.0	20	35
$MnPS_3$	$C_{12}TMA$ [a]	120	1.5	6.3	435

[a] $C_{12}TMA$ = dodecyltrimethylammonium.

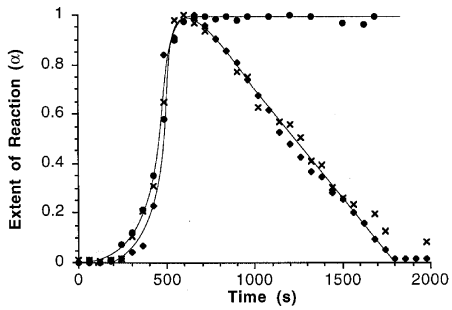

Fig. 3. Plot of extent of reaction (α) vs. time for the following reactions: (●) $C_{12}TMABr$ with $MnPS_3$ in water at 120°C; (×) $C_{16}TMABr$ with $MnPS_3$ in water at 120°C; (♦) $C_{18}TMABr$ with $MnPS_3$ in water at 70°C. $\alpha = I_{hkl}(t)/I_{hkl}(t = I_{max})$ for the (002) Bragg reflection in each case.

compound. The X-ray diffraction pattern of the product can be indexed on a hexagonal unit cell with a *c*-lattice parameter of 11.26 Å. Integration of the (001) Bragg reflection with respect to time is shown in Fig. 3. The half-life for the reaction at 120°C is ca. 400 s with the reaction essentially complete in 700 s. The increase in the interlamellar spacing of 4.77 Å is consistent with the packing of the dodecyltrimethylammonium ions parallel to the planes of the host lattice (Fig. 4). Elemental analysis is consistent with a formulation of this intercalate as $Mn_{0.92}PS_3(C_{12}TMA)_{0.16}$.

However, dramatically different behaviour was observed when we monitored the intercalation of the larger hexadecyl- and octadecyltrimethylammonium bromides ($C_{16}TMABr$ and $C_{18}TMABr$) in $MnPS_3$. For both reactions, we observed the growth of a series of Bragg reflections which can be indexed to a unit cell with *c*-lattice parameters of 33.8 and 36.2 Å for the hexadecyl- and octadecyltrimethylammonium reactions, respectively. These large *c*-lattice parameters correspond to interlayer expansions of ca. 27.3 and 29.7 Å for the hexadecyl- and octadecyltrimethylammonium intercalates, respectively. A plot of the time dependence of the integrated intensities of the Bragg reflections due to these intercalate phases shows that the initial rates of intercalation of all three ammonium cations are essentially equal, suggesting that the rate-determining step in each of these reactions is the separation of the $MnPS_3$ layers. However, for reactions involving the intercalation of $C_{16}TMA^+$ and $C_{18}TMA^+$, the peak intensities of the intercalate phases start

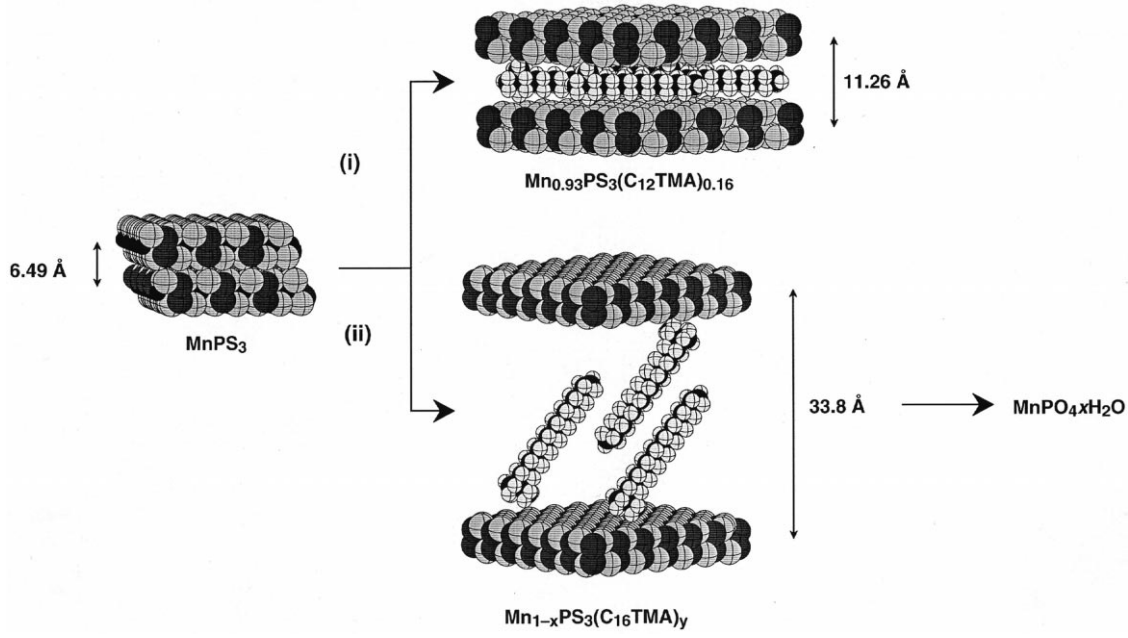

Fig. 4. Synthesis of long chain ammonium intercalates of $MnPS_3$: (i) $MnPS_3$ (150 mg) + $C_{12}TMABr$ (1 mmol) in 5 cm^3 water at 120°C, (ii) $MnPS_3$ (150 mg) + $C_{16}TMABr$ (1 mmol) in 5 cm^3 water at 120°C.

to decrease gradually after ca. 600 s and after approximately 30 min no reflections are observed in the energy window of the detector (Fig. 5). The resulting grey powder which can be collected from the reaction mixtures is identical from both reactions and is poorly crystalline. Both elemental microanalysis and X-ray microprobe analysis suggest that it has composition $MnPO_4 \cdot xH_2O$ although the unit cell dimensions do not match any of the known manganese phosphates or hydrogen phosphates.

Intercalation of the intermediate length tetradecyltrimethylammonium bromide (C_{14}TMABr) in $MnPS_3$ gives rise to a complex reaction. Different behaviour has been observed when the reaction was monitored in situ on three different occasions. The first attempt showed the transient formation of a new phase which could be indexed with a *c*-lattice parameter of 31.6 Å; on a second occasion a different phase was observed with a *c*-lattice parameter of 11.5 Å, which co-formed with a small amount of the previous phase. On another occasion only the phase with a 11.5 Å lattice parameter could be detected. A plot of the unit cell dimension versus the number of carbon atoms for the guest molecule, C_nTMA^+ ($n = 14$, 16, and 18), is linear. The gradient of this plot is 1.15 Å per C. Assuming the guest molecules form a monolayer between the $MnPS_3$ layers, then this suggests that the guest ions are oriented at ca. 65° to the host layers. In addition, it seems reasonable to postulate that the C_{14}TMA cation is just at the critical length where the energy difference between the guests lying parallel to the host layers or at an angle of 65° to the layer plane is very small.

2.2. Kinetics of intercalation of cobaltocene into lamellar metal chalcogenide hosts

Redox-active organometallic compounds can be intercalated into the metal dichalcogenides either by direct reaction, ion-exchange, or by electrochemical routes [25]. This significant reaction was first reported in 1975 when Dines described the intercalation of the metallocenes cobaltocene ($Co(Cp)_2$; $Cp = \eta$-C_5H_5) and chromocene ($Cr(Cp)_2$) into a range of metal disulfides (MS_2: M = Ti, Zr, Nb, Ta and Sn) [26,27]. Since then these materials have been extensively studied due to their fascinating structural and electronic properties. In general, the ability of an organometallic molecule to intercalate in a layered lattice has been based on empirical rules. Therefore we were excited at the possibility of being able to determine quantitatively the kinetics of these reactions and also of being able to investigate whether intermediate novel phases are formed during the course of the reaction.

We have investigated the kinetics of intercalation of $Co(Cp)_2$ into a range of layered metal dichalcogenides using in situ time-resolved EDXRD [19,28]. We were particularly interested to determine whether the variation in the rates of these intercalation reactions could be correlated with the chemical properties of the hosts. Fig. 6 summarises the extent of reaction $\alpha(t)$ versus time (t) for the intercalation of $Co(Cp)_2$ into ZrS_2, SnS_2, $SnSe_2$ and 2H-TaS_2. In each case

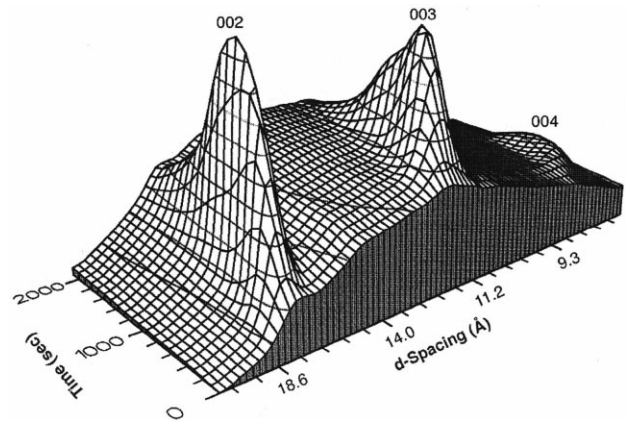

Fig. 5. Time-resolved energy dispersive X-ray diffraction of the reaction of C_{16}TMABr with $MnPS_3$ in H_2O at 120°C.

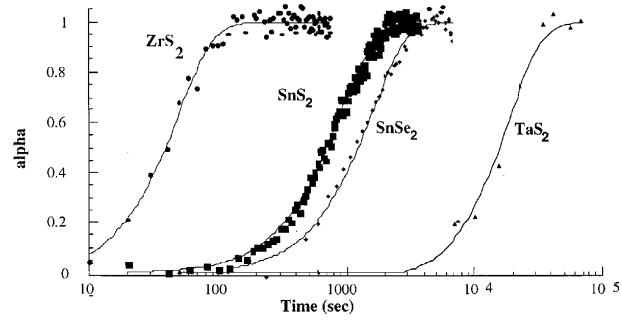

Fig. 6. Extent of reaction (α) vs. time for intercalation of $Co(Cp)_2$ into a range of metal dichalcogenides: ● ZrS_2, 8°C; ■ SnS_2, 20°C; ◆ $SnSe_2$, 50°C; ▲ $TaSe_2$, 120°C. The lines are fits to the Avrami deceleratory nuclei-growth model, $\alpha = 1 - \exp(-k(t - t_0))^{1.5}$.

the reaction yields first stage intercalation compounds of chemical composition $MX_2\{Co(Cp)_2\}_{0.30 \pm 0.05}$. In all cases we observed the smooth growth of intensity of the reflections due to the intercalate phases with increased *c*-lattice constants of 5.35 ± 0.02 Å. No intermediate phases of higher order staging are observed in any of these reactions. What is immediately striking about the data shown in Fig. 6 is the extreme variation in the rate of the reaction for each of the host lattices. For all the reactions, we tried to keep identical conditions; each host was sieved to a particle size distribution between 90–250 mm and the same amount of $CoCp_2$ solution was injected into each sample. Unfortunately, we had to vary the temperature of the reactions in order to collect data on a reasonable timescale. A summary of the rate constants (k_{obs} (s^{-1})) and half-life ($t_{1/2}$) for these reaction is shown in Table 2.

For SnS_2, ZrS_2 and $SnSe_2$ we have also investigated the rate of intercalation as a function of the initial $Co(Cp)_2$ concentration. In each case, varying concentrations of cobaltocene solution (enough volume to provide a 2:1 molar excess with respect to the host) were injected onto 200 mg of the host lattice at a convenient temperature for kinetic analysis. Fig. 7 shows each of the $\alpha(t)$ curves for the intercalation of cobaltocene into SnS_2 at 20°C for a range of initial $Co(Cp)_2$ concentrations.

Table 2
The half-lives and Avrami rate constants for the intercalation of $Co(Cp)_2$ into a range of lamellar metal dichalcogenides at 20 and 120°C (particle size 60–90 μm, in dimethoxyethane)

Host	20°C		120°C	
	Half-life (s)	$k\times10^3/s^{-1.5}$	Half-life (s)	$k\times10^3$ ($s^{-1.5}$)
ZrS_2	23	34.1	<5	400–600 [a]
2H-SnS_2	475	1.64	31	25.3
2H-SnSSe			225	
2H-$SnSe_2$	6730	0.12	410	1.92
2H-TaS_2			16000	0.05
2H-$NbSe_2$			2960	0.26
1T-TaS_2			>16000	<0.05 [b]
TiS_2			>60000	<0.01

[a] At 120°C this is too fast to measure accurately with the time resolution available; the range of values for k is an estimate based on extrapolation of lower temperature results.
[b] Shortage of beam time prevented full analysis. The reaction was significantly slower than that of 2H-TaS_2.

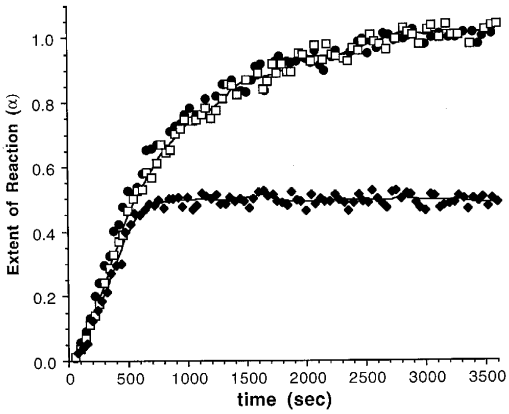

Fig. 7. Extent of reaction vs. time for the intercalation of $CoCp_2$ into SnS_2 at 20°C for a range of guest stoichiometries; the data are extracted from integration of the host (001) reflection such that $\alpha=1$ corresponds to complete loss of coherent diffraction from the host lattice. Data shown are for guest:host molar ratios of 1:1 (●), 0.33:1 (□) and 0.1:1 (♦).

Data could be fitted to Eq. (2) and, for the complete range of initial $Co(Cp)_2$ concentrations studied (10–70 mg cm^{-3}), the measured rate constants and half-lives are invariant within experimental error. Therefore, we conclude that the nucleation and diffusion rate are independent of $Co(Cp)_2$ concentration over the range investigated. The invariance on guest concentration and the congruency of the reaction kinetic curves suggest a number of issues. Firstly, the similarity in the sigmoidal nature of the extent of reaction curve for each system implies a consistent mechanism and a consistent ratio between the rates of nucleation and diffusion. Secondly, the diffusion of guest molecules to the host surface is insignificant with respect to the reaction rate.

If this is an example of a more general phenomenon, this observation has significant practical implications. The zero-order dependence in the guest concentration means that in future experiments it should not be necessary to use a large excess of guest molecules to expedite these reactions. This would be especially useful if the guests are expensive or particularly difficult to synthesise.

2.3. Kinetics of intercalation of lithium salts in aluminium hydroxide

The intercalation of LiCl in Gibbsite (γ-$Al(OH)_3$) is a remarkable example of an intercalation reaction in which both the cation and the anion are simultaneously intercalated in the host lattice [29–32]. The product of the reaction is $[LiAl_2(OH)_6]Cl\cdot H_2O$ which is a layered double hydroxide with a well ordered structure [33–35]. We have studied this reaction using time-resolved in situ EDXRD. In all cases the reactions proceeded directly to the first stage intercalation product and no other crystalline intermediate phases were observed. A typical set of in situ EDXRD spectra for intercalation of LiCl are shown in Fig. 8. The major peak that is observed to grow with time in this energy window corresponds to the (002) Bragg reflection of $[LiAl_2(OH)_6]Cl\cdot H_2O$ at $E=49.1$ keV ($d=7.65$ Å) while the (001) Bragg reflection of Gibbsite at $E=77.0$ keV ($d=4.85$ Å) decays in intensity. We can resolve no changes in the peak position or peak width at half maximum during the growth of the intercalate Bragg peaks. This is probably not too surprising

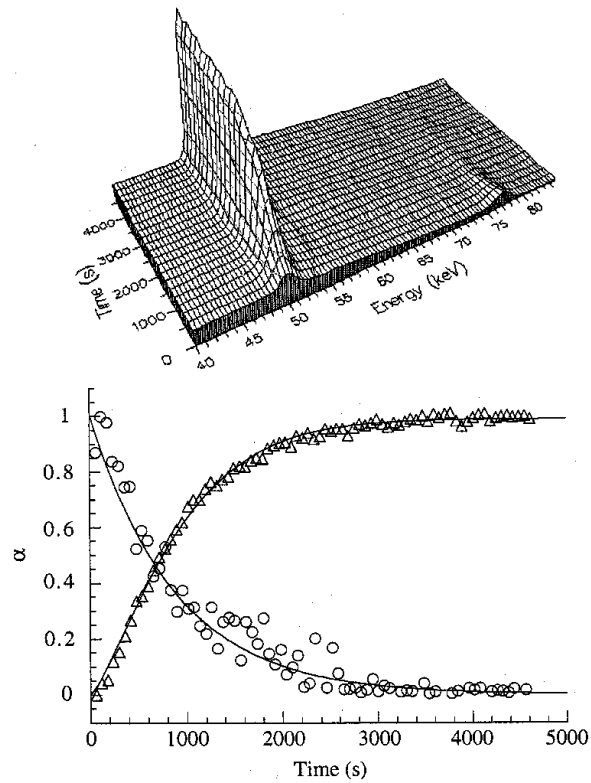

Fig. 8. (a) Time resolved in situ energy dispersive X-ray powder diffraction data showing the course of the reaction between Gibbsite and a 7.5 M aqueous solution of LiCl at 120°C giving $[LiAl_2(OH)_6]Cl\cdot H_2O$. (b) Plot of extent of reaction (α) of the (001) Bragg reflection ($E=77.1$ keV, $d=4.85$ Å) of the Gibbsite (○) and the (002) Bragg reflection of $[LiAl_2(OH)_6]Cl\cdot H_2O$ ($E=49.1$ keV, $d=7.65$ Å) (△) as a function of time.

given that the detector momentum resolution using post sample molybdenum slits is typically $\Delta E/E = 0.0115$.

Kinetic information was extracted from each experiment by integration of the (002) Bragg reflection of $[LiAl_2(OH)_6]Cl \cdot H_2O$. The errors on the integrated areas are small and contained within the data points. The integrated intensities were subsequently converted to the extent of the reaction (α) using the relationship Eq. (1): least-squares fits of the $\alpha(t)$ data are to the Avrami–Erofe'ev rate expression (Eq. (2)). We have investigated the rate of intercalation of LiCl in Gibbsite as a function of both temperature and LiCl concentration.

2.3.1. Effect of temperature

The temperature dependence of the intercalation reaction between a 10 M aqueous solution of LiCl and Gibbsite was investigated over the range 60–140°C. Fig. 9 plots the extent of reaction against time for the temperatures studied and it is clear that the rate of reaction has a marked temperature dependence. In each case the Avrami–Erofe'ev equation (Eq. (2)) has been fitted to the data. Furthermore, plots of reduced time ($t/t_{0.5}$) versus extent of reaction for the different temperatures are superimposable within experimental error, implying a consistent mechanism for the intercalation reaction over the whole temperature range.

The Avrami exponents obtained from the least-squares fits for all the data sets fell in the range 0.8–1.2, though a value of $m = 1.0$ gives a satisfactory fit to the majority of the experimental results. Assuming Avrami–Erofe'ev kinetics to be relevant, this indicates a two-dimensional diffusion controlled nucleation-growth model following instantaneous nucleation. In this case the Avrami–Erofe'ev equation becomes $\alpha = [1 - \exp(-kt)]$.

The validity of Eq. (2) for the whole process can be confirmed by a Sharp–Hancock analysis. In each case this analysis yields a single straight line over the whole reaction, implying that the Avrami–Erofe'ev kinetics discussed above are a good description of this system. Further evidence for this model can be obtained by consideration of the intersection of the host and intercalate curves. The intersection is at $\alpha = 0.5$, implying that loss of coherent diffraction from the host is matched by gain in coherence of the product. In cases where nucleation is random, the rate of loss of coherent diffraction from the host lattice exceeds the rate of growth of the product phase leading to the intersection being at $\alpha < 0.5$.

From the kinetic data obtained from the above analysis, it is possible to extract an activation energy for the intercalation of LiCl into Gibbsite using the Arrhenius expression, $k = A\exp(-E_a/RT)$. A plot of ln k versus $1/T$ yields a value of $E_a = 27$ kJ mol^{-1}. This compares with a value of $E_a = 41$ kJ mol^{-1} obtained from a study of the temperature dependence of the rate of intercalation of cobaltocene ($Co(\eta\text{-}C_5H_5)_2$) in SnS_2.

2.3.2. Effect of concentration

The effect of LiCl concentration on the intercalation reaction was studied at 120°C over the range 4–20 M. The reaction

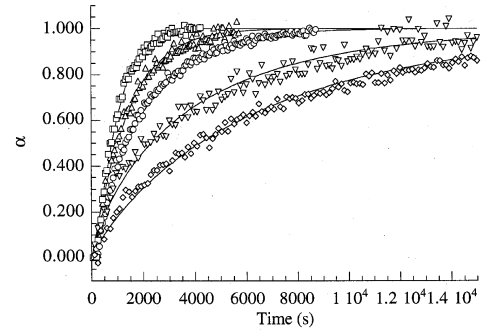

Fig. 9. Extent of reaction (α) against time (t) for the intercalation of LiCl into Gibbsite over a range of temperatures: 140°C (□), 120°C (△), 100°C (○), 80°C (▽) and 60°C (◇). Data for 110°C and 90°C have been omitted for clarity. The data have been fitted using the Avrami–Erofe'ev equation.

with 4 M LiCl did not go to completion in 4 h and no reactions were observed in 2 h for concentrations below this level. From the plots of extent of reaction against time shown in Fig. 10 it can be seen that the reaction rate is strongly dependent on the initial concentration of LiCl. In each case the Avrami–Erofe'ev equation has been fitted to the data. The observation of a dependence of rate of the reaction on the concentration of the guest is in contrast to previous studies on the intercalation of metallocenes into metal dichalcogenides which were found to be zeroth order with respect to the guest concentration. As for the temperature dependence reactions, plots of extent of reaction against reduced time are superimposable within experimental error, suggesting that the same mechanism is occurring in each case. This can be further confirmed by analysis of the Avrami exponents obtained from the curve fitting and from the Sharp–Hancock plots which lie in the range 1.0–1.5 though taking a value of 1.0 again gives a satisfactory fit to the majority of the data. This indicates a two-dimensional diffusion controlled nucleation-growth model following instantaneous nucleation, as was observed for the temperature dependence data. The kinetic parameters are summarised in Table 3.

The order of reaction with respect to LiCl concentration can be determined from a plot of ln k against ln[LiCl] which is shown in Fig. 11. The gradient of this plot is 0.52, indicating

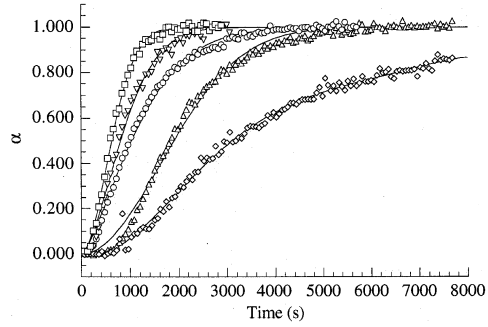

Fig. 10. Extent of reaction (α) against time (t) for the intercalation of LiCl into Gibbsite over a range of initial guest concentrations: 20 M (□), 15 M (▽), 10 M (○), 5 M (△), and 4 M (◇). Data for 12 M and 7.5 M guest solutions have been omitted for clarity.

Table 3
Summary of the kinetic parameters obtained from the Sharp–Hancock analysis of the intercalation of LiCl into Gibbsite for varying initial LiCl concentrations

[LiCl] (mol^{-1})	m [a]	k (s^{-1}) [b]	$t_{0.5}$ (s)
20	1.47	1.21×10^{-3}	600
15	1.40	1.09×10^{-3}	780
12	1.27	9.16×10^{-4}	900
10	1.00	7.40×10^{-4}	960
7.5	1.37	6.86×10^{-4}	1050
5	1.45	6.16×10^{-4}	1830
4	1.26	2.89×10^{-4}	3180

[a] From a least-squares fit to Eq. (2).
[b] From a least-squares fit to $\alpha = [1-\exp(-kT)]$.

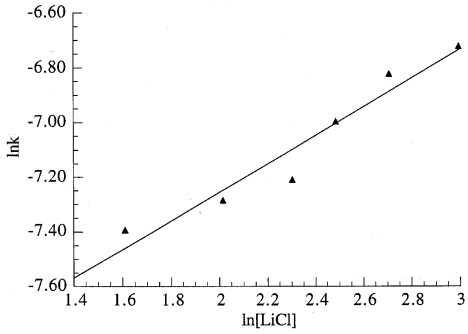

Fig. 11. Plot of ln k vs. ln[LiCl] used to determine the order of reaction with respect to the concentration of LiCl.

that the reaction is half order with respect to [LiCl]. This gives the rate equation as:

$$\text{rate} \propto k[\text{LiCl}]^{0.5}$$

2.4. Intercalation of ammonium ions in the layered silicate kanemite

The synthesis of mesoporous materials has been one of the most topical and rapidly moving fields in solid state chemistry of the last decade. The mechanism of formation of these materials is very poorly understood but is clearly an important issue. The synthetic approach originally reported by Kresge et al. [36] led to the development and investigation of the M41S family of mesoporous molecular sieves [37–39]. The three phases obtained from the M41S synthesis methods are hexagonal (MCM-41), cubic (MCM-48), and lamellar (MCM-50), of which the microscopy and diffraction data are reminiscent of surfactant/water binary systems. Beck et al. initially proposed a liquid crystal template (LCT) mechanism [37]. This mechanistic model served to illustrate the concept of aggregate molecular templating, but was quickly modified to include the role of the silicate anionic species. This model is better described as a process of cooperative assembly, as a result of favourable electrostatic interactions at the inorganic–organic interface [37,40–43].

Another approach, developed by Kuroda and co-workers, takes advantage of the ability of long chain alkyltrimethylammonium cations to intercalate into the single layered polysilicate, kanemite. This was an extension of the intercalation chemistry originally reported by Beneke and Lagaly [44]. Kuroda and co-workers initially reported that the formation of the silicate-surfactant complex [45,46], followed by removal of the surfactant, led to the formation of a hexagonal mesoporous silicate [47,48]. These materials can be tailor made with single size distribution channels in the range 20–40 Å. The mesoporous silicate material denoted FSM-16 is produced by intercalation of hexadecyltrimethylammonium cationic surfactants, and the formation process is representative of the transformation of two-dimensional layers to a three-dimensional framework [49].

We have recorded time-resolved in situ EDXRD spectra following the addition of an aqueous solution of heaxdecyltrimethylammonium chloride ($C_{16}H_{33}N^{+}Me_3Cl^{-}$ = C_{16}TMACl) to kanemite ($NaHSi_2O_5\cdot 3H_2O$) at 70°C over a period of 3 h. The spectra are shown accumulated as a three-

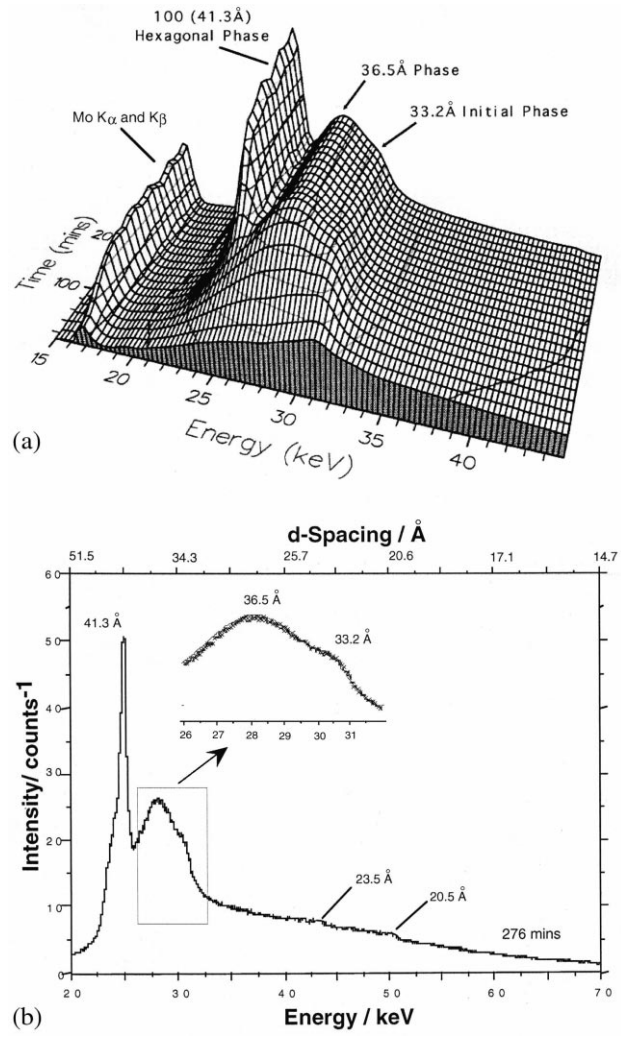

Fig. 12. (a) Three-dimensional stacked plot showing the energy dispersive powder X-ray diffraction spectra recorded following addition of 0.1 M hexadecyl-trimethylammonium chloride ($C_{16}TMA^{+}Cl^{-}$) to kanemite in water at 70°C. (b) The final in situ EDXRD spectrum taken after reaction completion, showing all observable diffraction features.

dimensional stacked plot in Fig. 12(a), along with the final spectrum recorded after 276 min (Fig. 12(b)) which clearly indicate the diffraction peaks present.

The stacked and single spectra can be described as a series of broad Bragg reflections viewed in energy space, that arise due to the growth of 'crystalline' silica-surfactant mesophases from the medium. A stirred suspension of kanemite at this pH and temperature showed only a broad featureless background, thus overwhelming X-ray scattering due to the silicate particles can be ruled out. We expect the coherent X-ray scattering at these low angles (high *d*-spacing) to produce broad Bragg reflections due to the convolution of the small ordered domain size of the silica-surfactant mesophases and the resolution function of the diffractometer setup.

Following the addition of the 0.1 M solution of C_{16}TMACl, a Bragg reflection grows in at a *d*-spacing of ca. 32 Å within 10 min. The *d*-spacing of this reflection increases gradually throughout the course of the reaction, reaching a constant value of 33.2 Å after 30 min. Subsequently, a second even broader Bragg reflection grows in with a *d*-spacing of ca. 36 Å, reaching a maximum after approximately 100 min. Once this Bragg reflection has reached its maximum intensity, we observe the growth of a series of reflections at *d*-spacings of 41.3, 23.5 and 20.5 Å. These reflections can be indexed as the (100), (110) and (200) Bragg reflections corresponding to a hexagonal symmetry mesophase ($a = 47.7$ Å, $2d_{100}/\sqrt{3}$). After pH adjustment with HCl to 8.5 to promote silanol condensation, filtration and calcination, FSM-16 is formed. The in situ diffraction data shown in Fig. 12(a) clearly show that the hexagonal (41 Å) silica-mesophase forms before dissolution of all the crystalline silicates.

It is highly likely that the intermediate phase with *d*-spacing of 33.2 Å has a layered, two-dimensional structure. A series of 00*l* reflections with *c*-lattice constant of 30.5 Å was observed in the laboratory X-ray powder diffraction pattern together with the Bragg reflections of the hexagonal phase from the untreated filtrate isolated after the reaction. It is reasonable to assume that the (00*l*) reflections belong to the lamellar phase observed by in situ EDXRD, and the increased *d*-spacing of the (001) reflection is due to swelling in the reaction medium. This has been observed in the intercalation chemistry of kanemite [50]. An interlayer separation of ca. 30 Å is consistent with intercalated $C_{16}TMA^+$ ions with an estimated length of ca. 23 Å and a silicate layer of approximately 6 Å thick. Lamellar phases appear to be common to all kanemite-surfactant reactions regardless of chain length. Recovery of this lamellar phase from the reaction mixture is possible by filtering the product before the reaction is complete and prior to addition of 1.0 M HCl. However, calcination of this sample led to a condensed amorphous phase, and collapse of any porous structure.

Given the current interest in template assisted crystallisation, these experiments clearly demonstrate the power of time-resolved, in situ diffraction measurements to monitor and help unravel the complex interactions of surfactant molecules with inorganic lattices. In this example, we have not only determined the kinetics of these reactions but also observed novel transient metastable phases that would probably have gone undetected using conventional laboratory procedures.

3. Conclusions

A range of environmental cells are now available to study the kinetics of intercalation into microcrystalline samples using time-resolved X-ray powder diffraction. The use of energy dispersive powder diffraction techniques enables reactions with half-lives of minutes to days to be examined. The design of the experiment allows a wide variety of solid–liquid reactions besides intercalation reactions to be studied with minimal turn-around time and experiments are currently underway to extend these opportunities to other classes of reactions.

Acknowledgements

We would like to thank the Leverhulme Trust, British Council, and the CIBA foundation for financial support and EPSRC for access to the Synchrotron Radiation Source, Daresbury Laboratory. We also thank Dr S.M. Clarke, Daresbury Laboratory and the technical staff at the SRS for helping in the design and construction of the experimental cell.

References

[1] J.G. Hooley, Carbon 11 (1973) 225.
[2] J.G. Hooley, Can. J. Chem. 40 (1962) 749.
[3] C. Riekel, Prog. Solid State Chem. 13 (1980) 89.
[4] C. Riekel, H.G. Reznik, R. Schollhorn, J. Solid State Chem. 34 (1980) 253.
[5] W. Paulus, H. Katzke, R. Schollhorn, J. Solid State Chem. 96 (1992) 162.
[6] C. Riekel, C.O. Fischer, J. Solid State Chem. 29 (1979) 181.
[7] C. Riekel, H.G. Reznik, R. Schollhorn, J. Solid State Chem. 34 (1979) 253.
[8] P. Barnes, Phase Transitions 39 (1992) 1.
[9] D. Hausermann, P. Barnes, Phase Transitions 39 (1992) 99.
[10] P. Barnes, S.M. Clark, D. Hausermann, E. Henderson, C.H. Fentiman, M.N. Muhamad, S. Rashid, Phase Transitions 39 (1992) 117.
[11] A.K. Sheridan, J. Anwar, Chem. Mater. 8 (1996) 1042.
[12] S.M. Clark, P. Irvin, J. Flaherty, T. Rathbone, H.V. Wong, J.S.O. Evans, D. O'Hare, Rev. Sci. Instrum. 65 (1994) 2210.
[13] S.M. Clark, J.S.O. Evans, D. O'Hare, C.J. Nuttall, H.V. Wong, J. Chem. Soc., Chem. Commun. (1994) 809.
[14] S.M. Clark, A. Nield, T. Rathbone, J. Flaherty, C.C. Tang, J.S.O. Evans, R.J. Francis, D. O'Hare, Nucl. Instrum. Methods Beam Interactions Mater. Atoms 97 (1995) 98.
[15] R. Clement, J. Am. Chem. Soc. 103 (1981) 6998.
[16] R. Clement, J.J. Girerd, I. Morgenstern Badarau, Inorg. Chem. 19 (1980) 2852.
[17] R. Clement, J. Chem. Soc., Chem. Commun. (1980) 647.
[18] J.S.O. Evans, D. O'Hare, Adv. Mater. 6 (1994) 646.
[19] J.S.O. Evans, S.J. Price, H.V. Wong, D. O'Hare, J. Am. Chem. Soc 120 (1998) 10837.

[20] S.F. Hulbert, J. Br. Ceram. Soc. 6 (1969) 11.
[21] M. Avrami, J. Chem. Phys. 7 (1939) 1103.
[22] M. Avrami, J. Chem. Phys. 8 (1940) 212.
[23] M. Avrami, J. Phys. Chem. 9 (1941) 177.
[24] B.V. Erofe'ev, C.R. Dokl. Acad. Sci. URSS 52 (1946) 511.
[25] D. O'Hare, in: D.W. Bruce, D. O'Hare (Eds.), Inorganic Intercalation Compounds, Inorganic Materials, Wiley, Chichester, 2nd edn., 1996.
[26] M.B. Dines, F.R. Gamble, B.G. Silbernagel, Bull. Am. Phys. Soc. (1975) 289.
[27] M.B. Dines, Science 188 (1975) 1210.
[28] S.J. Price, J.S.O. Evans, R.J. Francis, D. O'Hare, Adv. Mater. 8 (1996) 2989.
[29] A.P. Nemudry, V.P. Isupov, N.P. Kotsupalo, V.V. Boldyrev, Russ. J. Inorg. Chem. 31 (1986) 651.
[30] K.R. Poeppelmeier, S.-J. Hwu, Inorg. Chem. 26 (1987) 3297.
[31] M. Nayak, T.R.N. Kutty, V. Jayaraman, G. Periaswamy, J. Mater. Chem. 7 (1997) 2131.
[32] C.J. Serna, J.L. Rendon, J.E. Iglesias, Clays Clay Miner. 30 (1982) 180.
[33] I. Sissoko, E.T. Iyagba, R. Sahai, P.J. Biloen, Solid State Chem. 60 (1985) 283.
[34] J.P. Thiel, C.K. Chang, K.R. Poeppelmeier, Chem. Mater. 5 (1993) 297.
[35] A.V. Besserguenev, A.M. Fogg, S.J. Price, J.R. Francis, D. O'Hare, V.P. Isupov, B.P. Tolochko, Chem. Mater. 9 (1997) 241.
[36] C.T. Kresge, M.E. Leonowicz, W.J. Roth, J.C. Vartuli, J.S. Beck, Nature 359 (1992) 710.
[37] J.S. Beck, J.C. Vartuli, W.J. Roth, M.E. Leonowicz, C.T. Kresge, K.D. Schmitt, C.T.W. Chu, D.H. Olson, E.W. Sheppard, S.B. Mccullen, J.B. Higgins, J.L. Schlenker, J. Am. Chem. Soc. 114 (1992) 10834.
[38] J.S. Beck, J.C. Vartuli, G.J. Kennedy, C.T. Kresge, W.J. Roth, S.E. Schramm, Chem. Mater. 6 (1994) 1816.
[39] C.T. Kresge, J.C. Vartuli, W.J. Roth, M.E. Leonowicz, J.S. Beck, K.D. Schmitt, C.T.W. Chu, D.H. Olson, E.W. Sheppard, S.B. Mccullen, J.B. Higgins, J.L. Schlenker, Studies Surf. Sci. Catal. 92 (1995) 11.
[40] A. Firouzi, F. Atef, A.G. Oertli, G.D. Stucky, B.F. Chmelka, J. Am. Chem. Soc. 119 (1997) 3596.
[41] A. Monnier, F. Schüth, Q. Huo, D. Kumar, D. Margolese, R.S. Maxwell, G.D. Stucky, M. Krishnamurty, P. Petroff, A. Firouzi, M. Janicke, B.F. Chmelka, Science 261 (1993) 1299.
[42] Q.S. Huo, D.I. Margolese, U. Ciesla, P.Y. Feng, T.E. Gier, P. Sieger, R. Leon, P.M. Petroff, F. Schüth, G.D. Stucky, Nature 368 (1994) 317.
[43] A. Firouzi, D. Kumar, L.M. Bull, T. Beiser, P. Seiger, Q. Huo, S.A. Walker, J.A. Zasadzinski, C. Glinka, J. Nicol, D. Margolese, G.D. Stucky, B.F. Chmelka, Science 267 (1995) 1138.
[44] K. Beneke, G. Lagaly, Am. Miner. 62 (1977) 763.
[45] T. Yanagisawa, T. Shimizu, K. Kuroda, C. Kato, 56th Natl. Meet. of the Chemical Society of Japan, Tokyo, 1988, Abstract 1,761, No. IXIID42.
[46] T. Yanagisawa, T. Shimizu, K. Kuroda, C. Kato, Bull. Chem. Soc. Jpn. 63 (1990) 988.
[47] S. Inagaki, Y. Fukushima, K. Kuroda, J. Chem. Soc., Chem. Commun. (1993) 680.
[48] S. Inagaki, Y. Koiwai, N. Suzuki, Y. Fukushima, K. Kuroda, Bull. Chem. Soc. Jpn. 69 (1996) 1449.
[49] S. Inagaki, Y. Sakamoto, Y. Fukushima, O. Terasaki, Chem. Mater. 8 (1996) 2089.
[50] K. Kuroda, unpublished results.